

THE TANCO PEGMATITE AT BERNIC LAKE, MANITOBA.

IV. PETALITE AND SPODUMENE RELATIONS

PETR ČERNÝ AND R. B. FERGUSON

Department of Earth Sciences, University of Manitoba, Winnipeg

ABSTRACT

Crystals of petalite up to 2 metres in length occur in the upper intermediate quartz + spodumene + amblygonite (+ petalite) zone (5) adjacent to the pollucite body in the upper parts of the Tanco pegmatite. Petalite is frequently penetrated by fine-grained symplectites of spodumene and quartz, and by coarser aggregates of parallel spodumene fibers embedded in quartz. Euhedral tabular masses of these fibrous spodumene + quartz intergrowths also occur abundantly in the lower intermediate K-feldspar + albite + quartz + spodumene (+ amblygonite) zone (4).

Chemical analyses, densities, and quantitative x-ray powder diffractometer determinations show that the bulk composition of the spd + qtz intergrowths is close to that of petalite, and these results taken with the textural evidence show that the spd + qtz intergrowths originated by the breakdown of petalite. As shown by experimental data, this reaction was caused most probably by temperature decrease (Stewart 1963). The coarseness of the spd + qtz aggregates, the considerable volume reduction during their formation, and the consequent local migration of silica explain the deviations of their bulk compositions from that of petalite.

Another type of spodumene occurs as coarse columnar aggregates in the quartz cores (zone (7)). Some of this could be primary, but at least a part of it originated by recrystallization of the spodumene + quartz intergrowths. The only spodumene that is almost certainly primary is a third type that occurs in the central intermediate K-feldspar + albite + quartz (+ beryl + wodginite) zone (6), where it is intergrown with quartz in the interstices of the feldspars.

The physical properties and chemical compositions are presented for different petalite and spodumene varieties, and their alterations are described. The relations between petalite, spodumene, and pollucite both in nature and in experimental systems are discussed.

INTRODUCTION

The Tanco (Chemalloy) pegmatite at Bernic Lake in southeastern Manitoba contains, besides the tantalum minerals which are now being mined, and the well-known giant pollucite bodies, large amounts of lithium minerals. Figs. 2 and 3 in Crouse & Černý (1972) show that the spodumene-bearing and spodumene-rich zones constitute nearly half of the total volume of the pegmatite body. This spodumene has a very low iron content, and it thus has a potential use not only as a source of lithium but also for high refractory ceramics.

As well as being of potential economic value, the spodumene from the Tanco pegmatite is important from a petrological viewpoint. Most spodumene occurs as oriented intergrowths with quartz in aggregates whose outer shape strikingly resembles large crystals of petalite that have been found here recently in substantial amounts. (M. H. Froberg identified the first petalite specimens from this pegmatite in 1962; D. B. Stewart, pers. comm. 1971). This strongly suggests a close genetic relationship between these two minerals, and this may give information about the conditions under which the Tanco pegmatite originated. The present paper gives mineralogical data on the petalite and the spodumene, and describes their paragenetic relations leading to conclusions regarding their genesis.

OCCURRENCE

Petalite occurs mainly in the upper intermediate $\text{spd} + \text{qtz} + \text{amb}$ (+ pet) zone (5), particularly in the upper parts adjacent to the almost monomineralic pollucite zone (8) (see Figs. 2, 3 and list of zones in Crouse & Černý 1972). It forms log-shaped crystals up to 2 metres in length, imbedded in quartz and associated mainly with amblygonite-montebrazite, microcline-perthite, pollucite, and minor albite. Veinlets of fine-grained spodumene + quartz symplectites and parallel aggregates of fibrous spodumene intergrown with quartz penetrate most of the petalite crystals. Petalite is found also in the lower intermediate $\text{Kf} + \text{ab} + \text{qtz} + \text{spod}$ (+ amb) zone (4), but is rare in this assemblage, and it usually forms only patches within fibrous spodumene + quartz.

Three types of spodumene may be distinguished (besides the microscopic accessory spodumene found by Wright (1963) veining the pollucite bodies (8) and disseminated in the albitic aplite (3)) :

Type A — Tabular aggregates up to 2 metres across of waterclear, fibrous spodumene intergrown with quartz, with the spodumene fibers normal to the larger "faces" of the tabular masses. The spodumene fibers, occasionally flattened, range up to 10 cm in size. This type constitutes at least 90% of all the spodumene in the pegmatite, and it is found in zones (4) and (5).

Type B — Lath-shaped crystals of white spodumene, up to 1.5 metres in length, usually in slightly divergent bundles. These occur in the areas where zone (5) is transitional into the quartz cores (7), and in quartz-rich portions of zone (5) itself. This type has never been found in contact with, or in the close neighbourhood of, petalite.

Type C — Fibrous and columnar spodumene up to several cm in length, waterclear to pale greenish, embedded mostly in quartz, and inter-

stitial to microcline-perthite and albite in the central intermediate Kf + ab + qtz (+ ber + wod) zone (6). This type lacks the outer tabular shape of the spd + qtz intergrowths of the type A, although in some cases it is similar in texture.

MINERALOGY

Experimental methods

X-ray powder diffraction data were recorded on a Philips Norelco diffractometer using Cu/Ni radiation and $\text{CuK}\alpha_1 = 1.54051 \text{ \AA}$. In order to yield accurate spacings, fluorite annealed at 800°C ($a = 5.4620 \text{ \AA}$) was used as internal standard for the petalite patterns, but spodumene records were calibrated with quartz (using the 2θ values of Frondel 1962) because of coincidence of the usable fluorite peaks with spodumene reflections. Least squares refinements of the unit cell dimensions were performed by means of the self-indexing computer program of Evans *et al.* (1963), modified by D. E. Appleman.

For the quantitative phase analyses of the spd + qtz aggregates by x-ray powder diffractometry, the rotating sample holder was used. The intensities of the quartz reflection $10\bar{1}1$ and of the spodumene reflections $\bar{2}21$ and 310 were recorded six times for each of three different mounts of a single sample. The mounting technique of Bristol (1966) was used to minimize preferred orientation of the spodumene. The intensity ratio ($10\bar{1}1_{\text{q}} : \frac{1}{2}(\bar{2}21_{\text{s}} + 310_{\text{s}})$) was used to express the quantitative ratio of the two minerals, and this ratio was plotted on a calibration curve obtained by the same x-ray procedure from known mixtures of pure quartz and spodumene.

Densities were determined on a Berman torsion balance. Immersion liquids checked on the refractometer were used with sodium light to determine the refractive indices. Chemical analyses were carried out with the alkalis determined by atomic absorption spectrometry, $\text{H}_2\text{O}+$ by the Penfield method, and the remaining elements by x-ray fluorescence spectrography.

Petalite

This mineral forms large log-shaped to long tabular crystals. As far as can be concluded from rough measurements of interfacial angles and from the orientation of the characteristic cleavages (very good on $\{001\}$ and poor on $\{201\}$), the crystals show the usual forms and habit; they are prismatic along a , with $\{001\}$ and $\{010\}$ in the prism zone and $\{110\}$ and $\{201\}$ in the determination (*cf.* Deer *et al.* 1963a, p. 271). The colour is dark

grey to grey in fresh specimens, frequently transparent white. A milky or opaque white colour indicates incipient alteration.

Three specimens were selected for detailed study, a dark grey and a white material from a small crystal embedded in pollucite and quartz (BLM-50g and BLM-50w respectively), and another white sample from a giant crystal adjacent to pollucite (BLM-51). Chemical analyses of these three specimens are given in Table 1, where it may be noted that the specimen BLM-51 was found, on the basis of Cs content, to be contaminated by pollucite; this was confirmed by x-ray powder pattern. The admixture was deduced from the analysis using the composition of the Tanco pollucite published by Nickel (1961).

Recalculation of the chemical analyses based on 20 oxygens per unit cell gave formulae closely fitting the theoretical composition $\text{LiAlSi}_4\text{O}_{10}$

TABLE 1. CHEMICAL COMPOSITIONS OF PETALITE AND OF
SELECTED SPODUMENE + QUARTZ AGGREGATES

	Petalite			Spodumene + quartz		
	BLM-50 grey	BLM-50 white	BLM-51 ¹	BLM-51 recalc. ²	BLM-33	BLM-34
SiO ₂	77.85	77.60	76.85	77.66	77.10	77.05
Al ₂ O ₃	16.60	16.66	17.16	17.20	16.30	16.83
Fe ₂ O ₃	0.053	0.053	0.036	0.034	0.11	0.14
MgO	0.028	0.012	0.020	0.020	0.009	0.021
CaO	0.01	0.00	0.04	0.04	0.01	0.16
Li ₂ O	4.54	4.84	4.28	4.41	4.49	4.46
Na ₂ O	0.145	0.117	0.283	0.236	0.225	0.280
K ₂ O	0.050	0.040	0.280	0.287	0.063	0.032
Rb ₂ O	0.036	0.016	0.104	0.082	0.016	0.007
Cs ₂ O	0.136	0.021	0.977	—	0.005	0.010
H ₂ O ⁺	0.37	0.47	0.66	—	0.25	0.30
H ₂ O ⁻	0.13	0.11	0.13	—	0.08	0.10
P ₂ O ₅	0.03	0.04	0.03	0.03	0.05	0.05
	99.86	99.98	100.85	100.00	98.71	99.34

Analysts, K. Ramlal and R. M. Hill, 1969.

¹ Petalite contaminated by pollucite.

² Recalculated to 100% petalite by deducting the admixed pollucite on the basis of the Cs₂O content and the analysis of the Tanco pollucite in Nickel (1961).

($\text{Li}_2\text{O} \cdot \text{Al}_2\text{O}_3 \cdot 4\text{SiO}_2$), and showing no significant differences among the three specimens (Table 3). All are slightly deficient in silica which seems to be usual with petalite, but they show a much better occupancy of the lithium positions than do most of the relatively modern analyses collected by Deer *et al.* (1963a, p. 272). This contradicts the lithium-deficient formulae proposed by Comucci (1915; $\text{Li}_2\text{O} \cdot 2\text{Al}_2\text{O}_3 \cdot 4\text{SiO}_2$) and Mikkola & Wiik (1947; $4\text{Li}_2\text{O} \cdot 5\text{Al}_2\text{O}_3 \cdot 4\text{SiO}_2$), and is in agreement with the structure analysis of Zemmann-Hedlik & Zemmann (1955).

The optical properties agree well with those quoted in the literature for most petalites examined to date (Table 4); no specimen approaches the exceptionally high birefringence of the Hirvikallio petalite (Vesalio 1959). The specific gravities (Table 4) also compare well with most published values. The unit cell dimensions (quoted in Table 5) are close to those determined by Zemmann-Hedlik & Zemmann (1955); no powder reflections were found at around 15 Å, indicative of a doubled *c* period found by Gossner & Mussgnug (1928) and Tavora (1952).

Spodumene

Type A is fibrous, waterclear and colourless, and usually anhedral. In coarse aggregates, however, the fibers show predominant {100} and subordinate {110} in the prismatic zone. Type B is coarse columnar and shows the same forms in various extent and quality. Type C occurs as greenish stalks with cross-sections that are usually equant and with the form {010} in addition to {100} and {110}.

The chemical analyses of the spodumene specimens are given in Table 2. The only spodumene that could be obtained perfectly pure for chemical analysis is that of type B (specimens SPD-1, SPD-2A). The type A samples (BLM-33, BLM-34, SPD-2B) were recalculated from analyses of *spd* + *qtz* mixtures on the basis of the theoretical content of Al_2O_3 , 27.4 wt. %, and thus their unit cell contents (given in Table 3) should be taken with caution. Their main purpose is to enable one to compare directly the amounts of minor elements in A-type samples with those in the pure B-type samples. The iron and sodium weight percentages of the type C samples (BLM-11 and BLM-12) can be compared with those of types A and B in Table 2.

The A and B types show practically the same composition, with only negligible amounts of iron and sodium. Consequently, their optical properties and densities (Table 4), and their unit cell dimensions (Table 5) agree well with those published for other pure spodumenes (*cf.* Deer *et al.* 1963b, Haapala 1966). The partial analyses of the type C specimens show about the same contents of iron and sodium as the other types, but slight

changes in optical properties: the refractive index is slightly lower and the birefringence slightly higher than those of the types A and B.

It is worth mentioning that the analyses of spodumene B, and of Haapala's (1966) Haapaluoma spodumene, correspond to the theoretical $\text{LiAlSi}_2\text{O}_6$ composition much better than any of the analyses collected by Deer *et al.* (1963b). All the analyses are deficient in lithium and show, as noted by Deer *et al.*, some excess of silicon. Low lithium contents also characterize most of the Russian analyses of spodumene quoted by Vlasov *et al.* (1964).

RELATIONS BETWEEN PETALITE AND SPODUMENE

As mentioned in the second section, most petalite is penetrated by either fine-grained or fibrous spodumene, intergrown with quartz. The fine-grained veinlets are characteristic of specimens consisting largely of petalite, whereas the fibrous aggregates contain only small patches of petalite.

TABLE 2. CHEMICAL COMPOSITION OF SPODUMENE

	Type B			Type A		Type C	
	SPD-1	SPD-2A	SPD-2B ¹	BLM-33 ¹	BLM-34 ¹	BLM-11	BLM-12
SiO_2	63.45	63.20	63.93	63.68	63.72		
Al_2O_3	27.40	27.68	27.40	27.40	27.40		
Fe_2O_3	0.053	0.087	0.053	0.18	0.22	0.15	0.35
MgO	0.012	0.013	0.016	0.015	0.034		
CaO	0.16	0.00	0.00	0.02	0.26		
Li_2O	7.87	7.80	8.01	7.55	7.10	7.32	7.50
Na_2O	0.114	0.125	0.148	0.378	0.450	0.25	0.21
K_2O	0.038	0.019	0.035	0.106	0.052		
Rb_2O	0.002	0.001	0.006	0.026	0.012		
Cs_2O	0.001	0.001	0.002	0.008	0.016		
H_2O^+	0.30	0.36	0.28	0.42	0.49		
H_2O^-	0.11	0.08	0.08	0.13	0.16		
P_2O_5	0.02	0.03	0.04	0.08	0.08		
	99.53	99.40	100.00	100.00	100.00		

Analysts, K. Ramlal and R. M. Hill, 1969.

¹ Recalculated from analyses of samples containing quartz, on the basis of ideal Al_2O_3 content 27.4 wt.% of $\text{LiAlSi}_2\text{O}_6$, and adding SiO_2 to 100%.

The veinlets follow predominantly the two cleavages of petalite (Figs. 1 and 2), and consist of roughly equidimensional skeletal crystals of spodumene finely intergrown with quartz, which are not apparent without crossed nicols. Each mineral usually shows a uniform optical orientation in a single symplectite, even when its individual grains seems to be isolated by the other phase. The patchy symplectites show neither preferred orientation, nor any obvious crystallographic relationship to the host petalite.

The parallel aggregates of fibrous spodumene are also intergrown with grainy quartz (Fig. 3). The spodumene displays a strict parallelism with respect to the *c* (fiber) axis, but the *a* and *b* axes show considerable divergence, although mostly concentrated around a preferred setting. In the few specimens where the spodumene-petalite relation could be unambiguously established, the spodumene fibers were found to be oriented parallel to both cleavages and optical *Z* of petalite; thus *c* of spodumene is parallel to *b* of petalite.

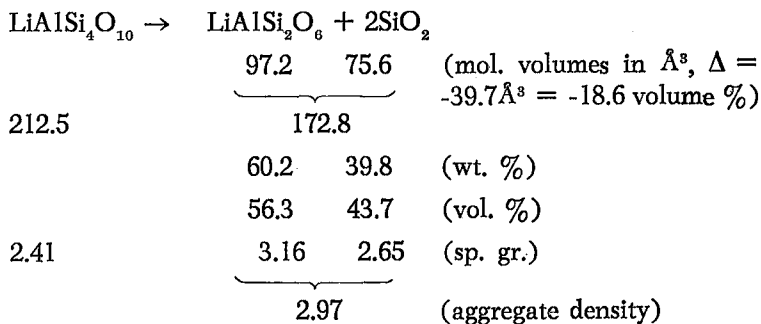
The fibrous *spd* + *qtz* aggregates showing a regular orientation to petalite are similar to the tabular masses of fibrous spodumene + quartz of the type A, the aggregation characteristic of the vast majority of spodumene in zones (4) and (5). The general resemblance in structure is strengthened as well by the outer shape of these *spd* + *qtz* intergrowths which frequently display the characteristic habit of petalite (Fig. 4). This

TABLE 3. UNIT CELL CONTENTS OF PETALITE AND SPODUMENE

	Li	Na	K	Rb	Cs	Ca	Mg	Al	Fe ³⁺	Si	P	
<i>Petalite</i>												
BLM-50 grey	1.870	.029	.006	.002	.006	.001	.004	2.006	.004	7.983	.003	
BLM-50 white	1.999	.023	.005	.001	.001	—	.002	2.016	.004	7.972	.003	
BLM-51	1.810	.047	.037	.005	—	.004	.003	2.070	.008	7.933	.027	
<i>Spodumene</i>												
Type B {	SPD-1	3.963	.027	.006	—	—	.021	.002	4.044	.005	7.950	.002
	SPD-2A	3.932	.030	.003	—	—	.002	4.091	.008	7.929	.003	
Type A {	SPD-2B	4.010	.036	.005	—	—	.003	4.020	.005	7.961	.004	
	BLM-33	3.801	.091	.017	.002	—	.002	.003	4.038	.017	7.967	.008
	BLM-34	3.565	.109	.008	—	—	.034	.006	4.049	.006	7.994	.008

Recalculated on the basis of 20 oxygens per unit cell of petalite, and 24 oxygens per unit cell of spodumene.

suggests a possible formation of all this spodumene and quartz by a breakdown of petalite, known already from other localities, which may be expressed as follows :



Ginzburg (1948) was the first author to explain by this reaction the close association of petalite and spodumene + quartz intergrowths, in the Kalbinsky Range, U.S.S.R., pegmatites. Other occurrences of these spd + qtz aggregates after petalite were described by Quensel (1948), Ginzburg & Gushtchina (1954), Staněk (1954), Vesasalo (1959), Neuvonen &

TABLE 4. PHYSICAL PROPERTIES OF PETALITE AND SPODUMENE

	α	β	γ	γ - α	Z/a ¹ Z/c ²	density	
<i>Petalite</i>							
BLM-50 grey	1.505	1.511	1.516	0.011	2°	2.42 ₀	
BLM-50 white	1.504	1.510	1.517	0.013	4°	2.39 ₉	
BLM-51	1.504	1.510	1.516	0.012	3°	2.41 ₄	
<i>Spodumene</i>							
Type A	BLM-33	1.661	1.666	1.676	0.015	26°	n.d.
	BLM-34	1.660	1.665	1.676	0.016	27°	n.d.
	SPD-2B	1.661	1.667	1.677	0.016	27°	n.d.
Type B	SPD-1	1.660	1.666	1.675	0.015	26°	3.153
	SPD-2A	1.661	1.667	1.677	0.016	25°	3.156
Type C	BLM-11	1.658	1.666	1.677	0.019	24°	n.d.
	BLM-12	1.659	1.665	1.678	0.019	25°	n.d.

¹ Petalite.

² Spodumene.

Vesalio (1960), Cooper (1964), and Hensen (1967); however, Quensel and Cooper did not recognize the nature and origin of these pseudomorphs.

The reaction was studied experimentally by Stewart (1963), who also examined the *spd* + *qtz* intergrowths from several localities (unpublished data; D. B. Stewart, private comm. 1969). Of 25 specimens of *spd* + *qtz* aggregates from the Tanco pegmatite, he found 19 to have densities between 2.75 and 3.00, and the remaining 6 have lower values (the ideal aggregate density is 2.97). He obtained similar data for material from Bikita and Varuträsk.

In the present study, we determined the phase composition of 14 *spd* + *qtz* intergrowths from zone (5) by quantitative *x*-ray powder diffraction. The results are shown in Fig. 5, and they indicate that most

TABLE 5. UNIT CELL DIMENSIONS OF PETALITE AND SPODUMENE

	<i>a</i> Å	<i>b</i> Å	<i>c</i> Å	β	
<i>Petalite</i>					
BLM-50g	11.777	5.129	7.632	113° 9'	
	± .010	± .005	± .004	± 3'	
BLM-50w	11.773	5.128	7.630	113° 9'	
	± .008	± .004	± .003	± 2'	
BLM-51	11.776	5.132	7.628	113° 2'	
	± .008	± .004	± .005	± 4'	
<i>Spodumene</i>					
Type A {	BLM-33	9.469	8.390	5.215	110° 12'
		± .003	± .002	± .005	± 2'
	BLM-34	9.466	8.394	5.218	110° 11'
		± .003	± .002	± .004	± 2'
Type B {	SPD-2B	9.469	8.387	5.216	110° 8'
		± .004	± .002	± .006	± 3'
	SPD-1	9.465	8.392	5.227	110° 5'
		± .004	± .002	± .006	± 4'
Type C {	SPD-2A	9.467	8.393	5.213	110° 9'
		± .004	± .002	± .006	± 3'
	BLM-11	9.456	8.392	5.211	110° 8'
		± .002	± .002	± .005	± 2'
Type C {	BLM-12	9.467	8.381	5.216	110° 12'
		± .003	± .002	± .006	± 3'

specimens contain quartz within $\pm 7\%$ of the amount required by the breakdown of petalite, with a tendency towards lower quartz percentages. Two specimens close to the theoretical spd/qtz ratio were chemically analyzed (Table 1) and found to be almost identical to petalite in composition. Characteristically, the spd + qtz aggregates are higher in sodium and show about the same content of iron as the parent petalite, as found also by Cooper (1964).

The textural and compositional data thus indicate that the tabular spd + qtz intergrowths in the Tanco pegmatite originated by the breakdown of petalite. This mode of formation also explains the remarkably low iron content of the spodumene. The petalite structure can incorporate only a limited amount of Fe^{3+} (most chemical analyses show only very few 0.X% Fe_2O_3 ; see also Table 1), and the spodumene produced by its breakdown inherits its low iron content. On the other hand, some sodium is probably introduced during the reaction; sodium and/or iron admixture is considered

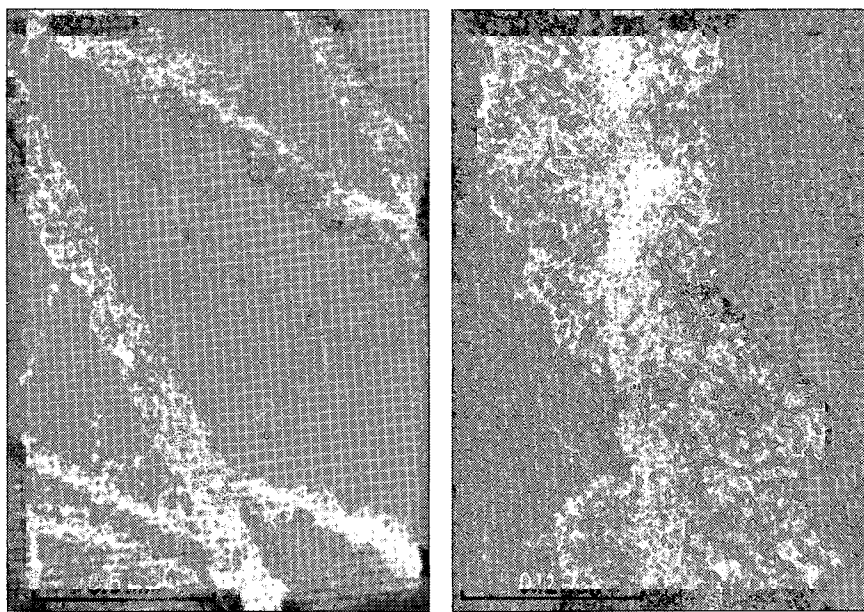


FIG. 1. Veinlets of the spodumene + quartz symplectite following the two cleavages of petalite. Thin section // to (010) of petalite, plane polarized light.

FIG. 2. Detail from Fig. 1, showing the spodumene + quartz aggregates growing irregularly from a straight cleavage fissure in petalite; the latter is clouded by cookeite and calcite. This section // to (010) of petalite, plane polarized light.

to be essential for spodumene crystallization in syntheses (Deer *et al.* 1963b).

Stewart's results quoted earlier indicated a higher quartz content in most aggregates than required by the reaction, and this may be explained by the volume relations in the reaction. The $\text{spd} + \text{qtz}$ aggregates show a volume reduction in relation to petalite, and this could be easily balanced by quartz enrichment. Quartz is the most abundant component of zone (5), and almost solely encompasses the petalite crystals and the $\text{spd} + \text{qtz}$ aggregates (Figs. 4, 6, 8, 9). The trends towards a lower quartz content in the specimens x-rayed by the present authors reflects an improper selection of samples: as realized later, the spodumene-enriched parts of the intergrowths are easier to collect in large one-piece specimens, particularly in the walls of the mine drifts, and thus it is likely that they were unconsciously favoured in sampling.

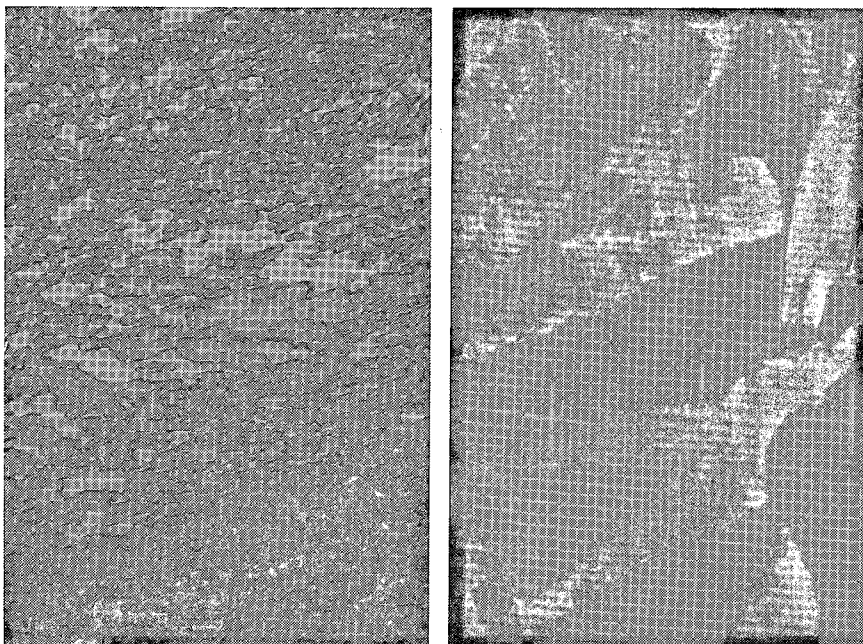


FIG. 3. A fine grained spodumene + quartz intergrowth showing a tendency of spodumene to form parallel fibrous aggregates. This section, plane polarized light.

FIG. 4. Wedge-shaped spodumene + quartz pseudomorphs after petalite in quartz, zone (5). Note the orientation of spodumene fibers normal to the longer edges of the intergrowths (upper right). The hammer head is 20 cm long.

The coarse crystals of the B-type spodumene, which are confined to the quartz-rich portions of zone (5) and to the quartz cores (7), may represent a primary spodumene, but at least some of them could also be secondary after petalite. Fig. 6 shows a cluster of coarse, slightly divergent spodumene blades that probably originated by recrystallization of the transected $spd + qtz$ intergrowth along a late fissure. Many similar relations have been observed in the underground workings.

The greenish C-type spodumene from zone (6) frequently forms sub-parallel aggregates embedded in quartz, but these give no indication of petalite morphology, and their compositions, as estimated visually in hand specimens, show broad variations. Furthermore, irregular groups of independent crystals are more a rule than an exception, the physical properties are slightly different and the iron content tends to be higher in some cases. For these reasons we consider this spodumene to be a primary phase.

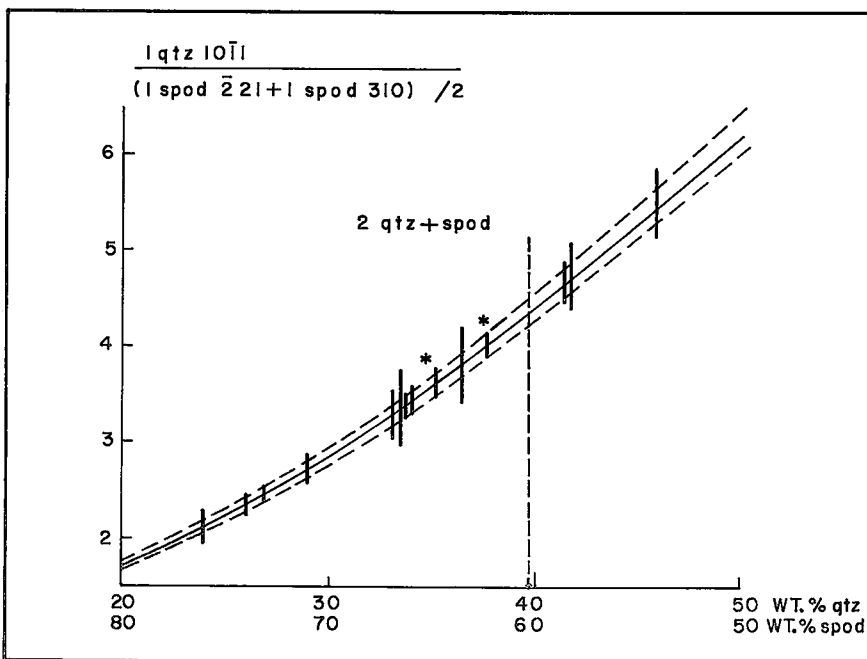


FIG. 5. Quantitative x-ray powder diffractometer determination of the phase composition of the spodumene + quartz intergrowths. The solid line is the best line through five calibration points, each of which was the mean of 18 separate records. The dashed lines subparallel to the calibration curve show the standard deviation of the standards. The dashed 2 qtz + spd line indicates the composition corresponding to that of petalite.

ALTERATION OF PETALITE AND SPODUMENE

Petalite is in places replaced by radiating, fan-shaped cleavelandite "stuffed" with tiny grains of quartz. Fine fibrous spodumene was found with some of these albite + quartz aggregates. Later alteration commonly produced adularia and cookeite in irregular patches and veinlets, and cookeite with calcite disseminated in microscopic grains throughout the petalite blocks. Massive, cleavage-controlled layers of adularia, cookeite, quartz, and calcite are rather exceptional.

Coarse spodumene of the B-type was not found altered. The fibrous spd + qtz aggregates (type A) are frequently cut by veinlets of albite finely intergrown with quartz, especially in the central parts of the albite crystals. Late alteration produced various assemblages consisting of albite, adularia, quartz, cesian analcime, cesian beryl, apatite, lithophosphate, montmorillonite-illite, and calcite (cf. Černý 1972b). The greenish spodumene of type C was occasionally found altered into a fine-grained mixture of cookeite, quartz and calcite.

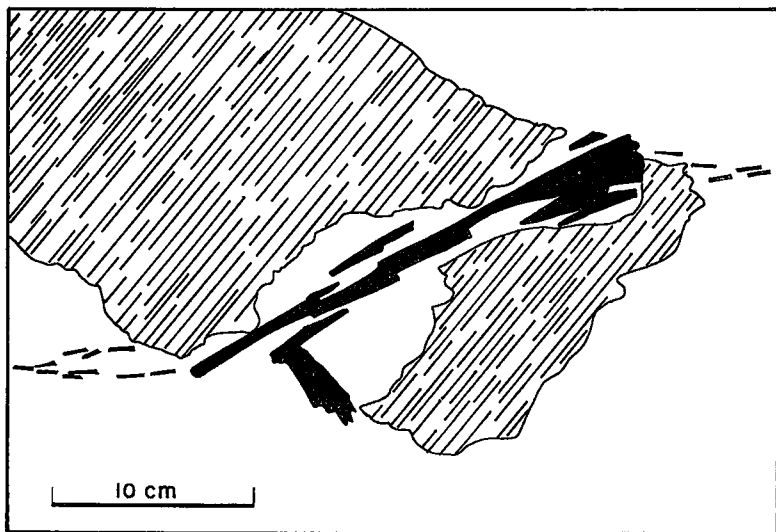


FIG. 6. A spodumene + quartz pseudomorph after petalite (striated) in quartz (white) of zone (5). The fibrous spd + qtz aggregate is cross-cut by coarse-bladed spodumene (black) and coarse quartz growing along a fissure visible in the neighbouring quartz.

DISCUSSION

The present work along with other related studies has established that petalite was the only primary lithium silicate in zones (4) and (5) (with the status of eucryptite uncertain; *cf.* Černý 1972a), and that it was later converted to spodumene + quartz. Some of these pseudomorphs were later recrystallized into coarse spodumene blades that occur in the quartz-enriched parts of zone (5) and in the quartz cores (7), but some of this spodumene could also be primary. Greenish spodumene from the feldspar interstices in zone (6) has most of the characteristics of a primary phase.

The p-T relationships of the crystallization interval of a lithium pegmatite are shown in Fig. 7 along with the stability field of petalite as determined experimentally (Jahns & Burnham 1958, Stewart 1963). Since the bulk lithium content of the Tanco pegmatite could be considered slightly higher than that of the Harding pegmatite used by Jahns & Burnham, its magmatic interval would be shifted to slightly lower temperatures (*cf.* Wyllie & Tuttle 1964 on the influence of Li on granitic melts). In any

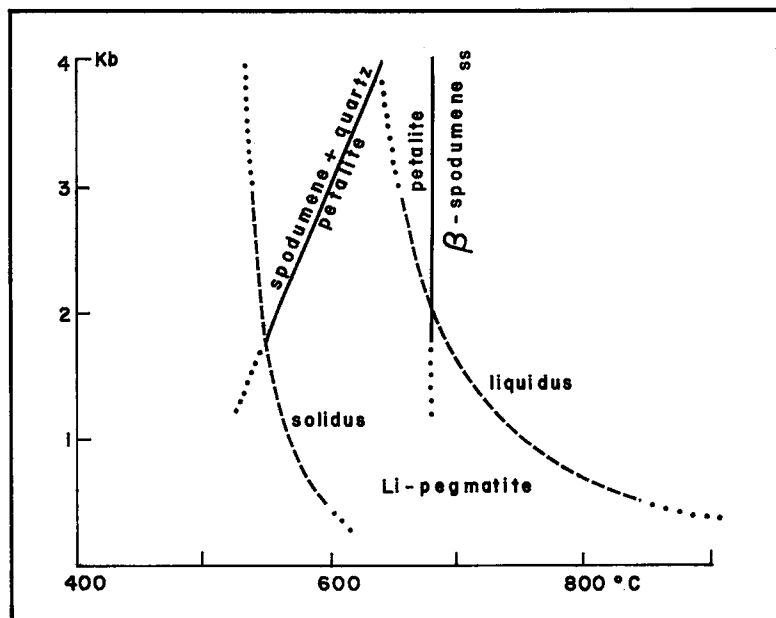


FIG. 7. Stability field of petalite, the spodumene + quartz region at higher pressures and lower temperatures (according to Stewart 1963, full lines), and the crystallization interval of the Harding, New Mexico, pegmatite (according to Jahns & Burnham, 1958, dashed lines); extrapolations dotted.

case, the stability field of petalite overlaps most of the magmatic crystallization range of a lithium-rich pegmatite, and the conversion of petalite into spodumene and quartz emerges as a consequence of temperature decrease, rather than a pressure rise within a very restricted temperature range.

This does not necessarily mean, however, that all the Tanco petalite crystallized from a magma. On the contrary, the textural and compositional relationships observed in the mine, particularly in the lower parts of zones (4) and (5), strongly suggest that it crystallized from a gaseous phase separated by resurgent boiling from an originally homogeneous melt (Fig. 8). Jahns & Burnham (1958, 1969) produced similar textures experimentally, and proved them to originate by magmatic crystallization of "residual" sodic aplite overlain by very coarse-grained quartz, K-feldspar and lithium silicates precipitated from a coexisting supercritical gas.

Stewart (1963, *priv. comm.* 1969) found that the assemblages crystallized from a supercritical fluid always show quartz predominating over feldspar. This is typical of the spodumene-rich (originally petalite-rich) zone (5) which consists mainly of quartz and $\text{spd} + \text{qtz}$ aggregates

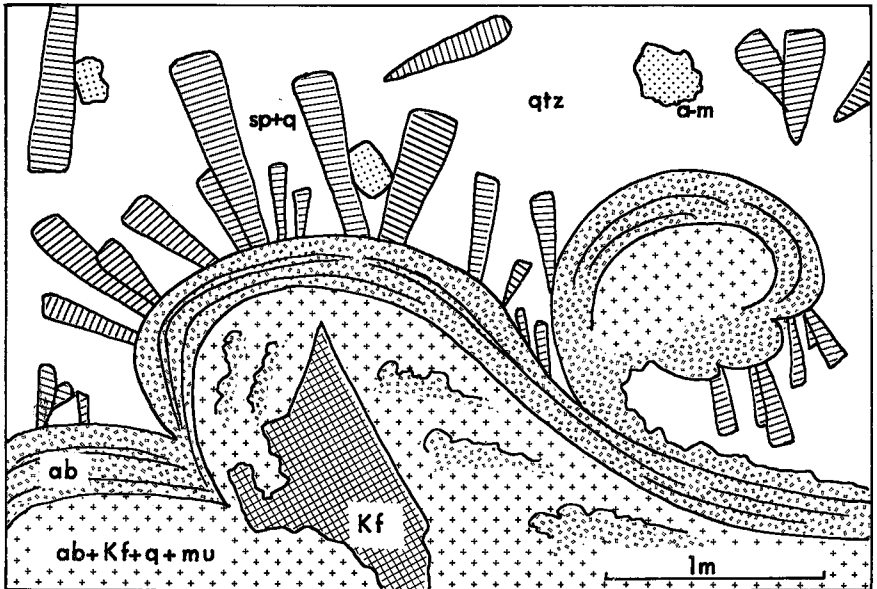


FIG. 8. A typical texture from the lower parts of the Tanco pegmatite, with the feldspathic wall zone ((2) — $\text{ab} + \text{Kf} + \text{qtz} + \text{mu}$) overlain by undulating albitic aplite ((3) — ab) and this encircled by a feldspar-poor "facies" of the intermediate zone ((4) — $\text{qtz} + \text{spd} + \text{qtz} + \text{a-m}$). Note the spodumene + quartz pseudomorphs after petalite radiating from the surface of the aplite into quartz.

(petalite) with subordinate amblygonite-montebbrasite and minor K-feldspar, pollucite, and albite; a typical example of amblygonite-montebbrasite and $\text{spd} + \text{qtz}$ pseudomorphs "floating" in quartz is shown in Fig. 9. (It must be stressed that the apparent crystallization sequence in this figure — petalite growing on amblygonite — is frequently reversed, and amblygonite-montebbrasite commonly occurs attached to petalite crystals or filling in irregular interstices among them.)

The first alteration of both petalite and spodumene was a replacement by albite. There is no evidence to indicate whether this metasomatism was a single event affecting both minerals simultaneously or a repeated reaction under different conditions. All late products — adularia, cookeite, cesian analcime, calcite, etc. — undoubtedly originated at very low temperatures under alkaline hydrothermal conditions, as discussed elsewhere (Černý 1972b).

All the possible implications of these petalite — spodumene relations and of the mode of petalite crystallization in relation to the general petrology of the Tanco pegmatite will be evaluated at a later date, after

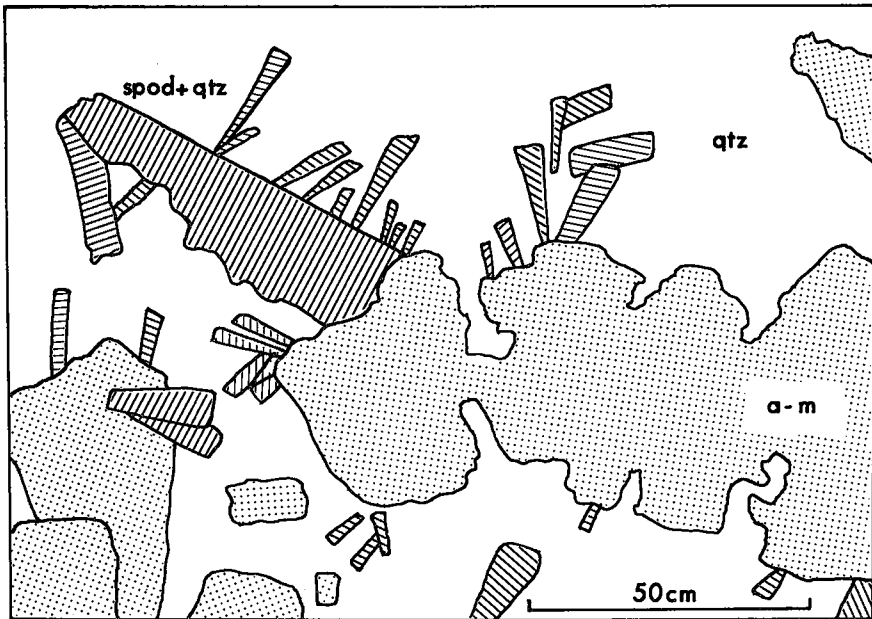


Fig. 9. A typical aggregation of amblygonite-montebbrasite and spodumene + quartz pseudomorphs after petalite, "floating" in quartz of the lower parts of the intermediate zone (5). The relative age of the spodumene + quartz pseudomorphs and amblygonite-montebbrasite is frequently reversed in other parts of the same zone.

additional data on other minerals and assemblages have been accumulated. At present, however, at least some general observations related to the petrology of petalite may be pointed out :

(i) Petalite has been described associated mainly with quartz and microcline-perthite in the Tanco pegmatite, in the upper parts of the Bikita, Southern Rhodesia deposit (Cooper 1964), in the pegmatites of Central Asia (Rossovskii & Klotchkova 1965), at Luolamäki, Finland (Mikkola & Wiik 1960 ; Neuvonen & Vesasalo 1960), and in the Nová Ves pegmatite in Southern Bohemia (Staněk & Čech 1958 ; J. Staněk, priv. comm. 1970). In the lower petalite-bearing zones of the Bikita pegmatite (Cooper 1964), and in the spodumene-rich zone of the Silverleaf lithium pegmatite in S.E. Manitoba (unpublished data by the authors), petalite and/or $\text{spd} + \text{qtz}$ are embedded in a matrix of quartz, Li-mica and albite, with albite constituting less than 10% of the whole assemblage ; in addition, K-feldspar is abundant in this association at Bikita. In pegmatites where petalite is associated mainly with albite, this feldspar has been found to be a late metasomatic product, replacing also K-feldspar (e.g. Staněk 1954, Neuvonen & Vesasalo 1960, Ginsburg & Gushtchina 1954, J. Staněk, priv. comm. 1970). The same relations seem to hold in the Varuträsk pegmatite, although Quensel's description does not present a clear picture of the general petalite-feldspar relations.

Thus petalite is found associated with either K-feldspar, or K-feldspar with minor albite, or it occurs in assemblages poor in both feldspars. It seems to prefer to be associated with K-feldspar, and where albite is abundant, it is always of later metasomatic origin.

The close association of petalite with K-feldspar is most probably caused by the physical nature and specific composition of the common parent medium. The quartz-rich coarse-grained assemblage of petalite, quartz and K-feldspar of the Tanco zone (5) is also typical of the upper parts and/or cores of the other petalite-bearing pegmatites referred to above, and this suggests a precipitation of these minerals from a supercritical gas in all of them (cf. Fig. 8). As shown by Jahns & Burnham (1958, 1969) and discussed by Jahns & Tuttle (1963), potassium and lithium are preferentially leached from a magma into a coexisting gaseous phase, whereas most of the sodium remains in the melt, and thus, control of the chemical composition of the parent medium over the crystallization of petalite seems improbable. Despite the lack of petalite + primary albite assemblages in nature, petalite can be crystallized without difficulty in sodium-rich laboratory systems producing coexisting albite (D. B. Stewart, priv. comm. 1970).

(ii) The usual association of petalite and pollucite has been known since the last century, although it is not as inviolable as suggested by the

petalite synonym castorite. In lithium pegmatites the conditions for the crystallization of petalite rather than some other lithium silicate are controlled mainly by temperature and pressure, whereas pollucite formation requires an exceptionally high concentration of cesium as an additional factor. Thus it is possible for petalite to occur alone in lithium pegmatites that were not sufficiently enriched in Cs to form pollucite. However, the concentration of Cs seems to occur preferentially in a low pressure environment, as shown by Melentjev (1961), and low-pressure pegmatites are those in which petalite could be expected (Fig. 7). Thus a low-pressure regime favouring cesium enrichment in a lithium pegmatite tends to produce the "mythological" petalite (castorite) — pollucite pair.

(iii) In petalite- and pollucite-bearing pegmatites in which most petalite has been converted to $\text{spd} + \text{qtz}$, the persisting petalite which survived breakdown and later alteration is found in the close neighbourhood of, or in immediate contact with, pollucite. The distribution of petalite in the Tanco pegmatite clearly shows this relation. The same relationship can be seen in the cross-sections of the Varuträsk pegmatite (Quensel 1956, Plate V, Fig. 2), and in some parts of the Bikita pegmatite (Cooper 1964, Fig. 3). While the reasons for this phenomenon are still obscure, and while there are undoubtedly other factors influencing the metastable persistence of petalite, the frequent close association of persisting petalite with pollucite must have some importance in the preservation of the former. (It is possible that some minor elements may stabilize the petalite structure, or that petalite may persist as a result of being shielded from fluids, or a local absence of sodium may be the answer; large petalite-bearing areas of the Bikita and Varuträsk pegmatites seem to carry no pollucite.)

(iv) Besides the most common blocky variety of petalite constituting economically important zones and originating at a relatively high temperature, other types of petalite are known that were formed under low-temperature and low pressure "alpine vein" conditions. Ginzburg & Gushtchina (1954) reported two late generations of petalite — one formed in open vugs at the expense of earlier spodumene and petalite together with adularia, quartz, and some albite, the other either coating this assemblage as fine needles or forming independent veinlets in the early minerals.

This suggests that petalite can not only exist below the lower temperature limit of its stability (as discussed above), but that it can also originate from hydrothermal solutions at very low p-T conditions. Because of sluggish reaction rates, it has not been possible to establish the petalite/spodumene + quartz boundary at pressures lower than 2 kb (D. B. Stewart, pers. comm. 1969). An extrapolation to lower pressures would leave the petalite field out of the temperature range of alpine vein crystallization

(400 — 200°C) even if the boundary curves gently towards lower temperatures (Fig. 7). However, a hydrothermal synthesis of petalite at 330 — 450°C was performed by Barrer & White (1951), and thus petalite has been shown to originate under these conditions, at least metastably.

(v) As shown earlier, the $\text{spd} + \text{qtz}$ pair forms either cleavage-controlled veinlets of seemingly unoriented patchy symplectites in petalite, or parallel fibrous aggregates that seldom contain any petalite relics. It is difficult to imagine that all the parallel fibrous aggregates had to pass through, and recrystallize from an earlier stage consisting of the unoriented patchy symplectites. It is more probable that the parallel fibrous material, overwhelmingly predominant over the other type, originated *en masse* and simultaneously during the initial temperature decrease below the limits of the petalite stability field in large parts of the petalite-bearing zones, and the patchy symplectites penetrated the surviving petalite later under different conditions.

Whatever the origin of these aggregates, the crystallographic control of the parent petalite over the orientation of the secondary fibrous spodumene ($c_{\text{spd}}//b_{\text{pet}}$) deserves further study, particularly because it seems to be strictly enforced despite the considerable volume reduction involved in the reaction.